Imaging rapid redistribution of sensory-evoked depolarization through existing cortical pathways after targeted stroke in mice

Albrecht Sigler[a,b], Majid H. Mohajerani[a,b], and Timothy H. Murphy[a,b,c,1]

[a]Department of Psychiatry, Kinsmen Laboratory of Neurological Research, [b]Brain Research Center, and [c]Department of Cellular and Physiological Sciences, University of British Columbia, 2255 Wesbrook Mall, Vancouver, BC, Canada V6T 1Z3

Edited by Michael M. Merzenich, University of California, San Francisco, CA, and approved May 26, 2009 (received for review December 19, 2008)

Evidence suggests that recovery from stroke damage results from the production of new synaptic pathways within surviving brain regions over weeks. To address whether brain function might redistribute more rapidly through preexisting pathways, we examined patterns of sensory-evoked depolarization in mouse somatosensory cortex within hours after targeted stroke to a subset of the forelimb sensory map. Brain activity was mapped with voltage-sensitive dye imaging allowing millisecond time resolution over 9 mm^2 of brain. Before targeted stroke, we report rapid activation of the forelimb area within 10 ms of contralateral forelimb stimulation and more delayed activation of related areas of cortex such as the hindlimb sensory and motor cortices. After stroke to a subset of the forelimb somatosensory cortex map, function was lost in ischemic areas within the forelimb map center, but maintained in regions 200–500 μm from blood flow deficits indicating the size of a perfused, but nonfunctional, penumbra. In many cases, stroke led to only partial loss of the forelimb map, indicating that a subset of a somatosensory domain can function on its own. Within the forelimb map spared by stroke, forelimb-stimulated responses became delayed in kinetics, and their center of activity shifted into adjacent hindlimb and posterior-lateral sensory areas. We conclude that the focus of forelimb-specific somatosensory cortex activity can be rapidly redistributed after ischemic damage. Given that redistribution occurs within an hour, the effect is likely to involve surviving accessory pathways and could potentially contribute to rapid behavioral compensation or direct future circuit rewiring.

brain plasticity | focal ischemia | in vivo imaging | recovery of cortical function | somatosensory cortex representation

The majority of those suffering a stroke will survive the initial insult, but will experience some form of sensory, motor, or cognitive impairment. Many will experience some restitution of function over the ensuing weeks to months after stroke. Evidence suggests that circuit changes within adjacent surviving regions of the brain may be critically involved in this recovery process (1–4). The extent of circuit reorganization in peri-infarct cortex correlates with recovery of cortical function lost after stroke (5, 6). Mechanisms suggested for mediating cortical reorganization involve the formation of novel circuits, the unmasking of existing, but latent, synaptic connections, and modulation of synaptic efficacy in active connections (7, 8). Although redistribution of circuit function is obviously the final outcome, in the first hours to days after stroke a competing process termed "diaschisis" may lead to reversible suppression of function in regions adjacent to and physiologically connected to the infarct (9, 10). We postulate that the distribution of residual function hours after stroke and its relation to local blood flow is a critical determinant of what circuits are available for future activity dependent plasticity over days to weeks after stroke.

Despite extensive study of sensory circuits days to weeks after stroke (2, 4, 11–14), relatively few studies address functional redistribution over shorter time scales. Electrophysiological studies showed hyperexcitability of peri-infarct regions in the somatosensory cortex within hours after stroke (15, 16), but were not able to map the flow of sensory signals over wide regions of brain. Here, we apply voltage-sensitive dye (VSD) imaging to examine changes in forelimb and hindlimb somatosensory maps that occur within hours after acute stroke. VSD imaging reveals cortical activity, not only in the form of sensory-evoked action potentials, but also propagating subthreshold changes in membrane potential through which the effects of sensory stimuli are propagated over large regions of brain (17, 18). Before stroke, we find that some forelimb stimulus derived sensory signals spread to related areas of brain such as hindlimb somatosensory cortex. Unexpectedly, after stroke to the forelimb area, these off-target forelimb derived signals can be preserved despite the loss of much of the forelimb map and provide a new center of forelimb map activity. Conceivably, this new forelimb area may provide signaling that directs future structural plasticity and subsequent reorganization of somatosensory cortex function over longer timescales.

Results

To examine the sensorimotor cortex activity and its temporal and spatial changes after acute stroke, we used established protocols for in vivo imaging under urethane anesthesia (19). A craniotomy over the right hemisphere of an adult mouse allowed us to record changes in cortical membrane potential in vivo by using the voltage-sensitive dye RH1692 (20) as described in the methods and in (21–23). To record responses in areas of the somatosensory cortex that represent the forelimb and hindlimb, the contralateral forelimb or hindlimb was stimulated with a single 5-ms movement by a piezoelectric device (scheme: Fig. 1*A*). To generate maps of the VSD responses (Fig. 1 *B* and *C*), we used thresholding to define map borders: Mapped activity was defined as pixels with at least a half maximal change in VSD fluorescence signal ($\Delta F/F_0$), normalized from baseline to its peak value. To create maps of surface blood flow we imaged laser speckle contrast (Fig. 1 *D* and *E*) as described (19, 24, 25).

We blocked blood flow in 1–3 middle cerebral artery fine branches (diameter $\leq$50 μm) that were thought to supply the anterior half of the forelimb representation by photoactivation of intravenously injected Rose Bengal (19, 26, 27) by using a custom-made focused laser light delivery system that can target photoactivation with resolution in vivo higher than 5 μm (25). Loss of blood flow was quantified by taking the difference between laser speckle images before and after occlusion (Fig. 1

Author contributions: T.H.M. designed research; A.S. and M.H.M. performed research; A.S. and M.H.M. analyzed data; and A.S. and T.H.M. wrote the paper.

The authors declare no conflict of interest.

This article is a PNAS Direct Submission.

[1]To whom correspondence should be addressed. E-mail: thmurphy@interchange.ubc.ca.

This article contains supporting information online at www.pnas.org/cgi/content/full/0812695106/DCSupplemental.

NEUROSCIENCE

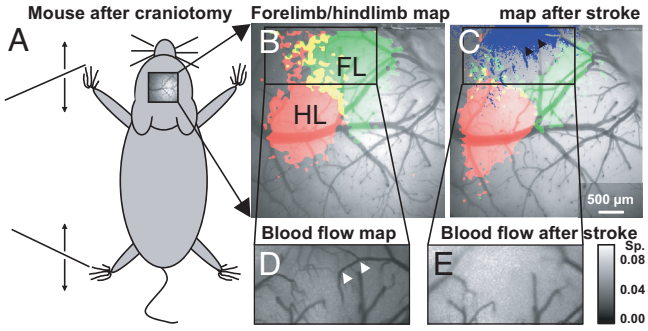

Fig. 1. Mapping sensory-evoked depolarization with VSD after stroke targeted to a subset of the somatosensory cortex. (*A*) Schematic showing C57 Bl6 mouse after craniotomy. The black lines at the left of the scheme represent moving shafts that stimulate the fore- and hindlimb. (*B*) Maps of VSD fluorescence changes indicating depolarization in the sensorimotor cortex in response to stimulation of forelimb (FL, green), hindlimb (HL, red), and the overlap of forelimb and hindlimb map (yellow). (*C*) Maps of VSD fluorescence as in *B* after photothrombotic stroke targeted to arterioles indicated by black arrows. Loss of blood flow (determined from the difference of speckle signals as shown in *D* and *E*) overlaid as blue shade. (*D*) Laser speckle image to determine blood flow (area in *B*). Darker tones indicate higher velocity blood flow. (*E*) Laser speckle image showing that blood flow was blocked at positions indicated by arrows in *D*. (Calibration bar indicates speckle contrast; Sp, standard deviation/mean.)

D and *E*). To assess functional deficits, we performed VSD mapping again in response to stimulation of the contralateral limbs. Focal stroke reduced function in at least half, but not all, of the forelimb area, and in some cases parts of the hindlimb map were also affected. The area of stroke-related function loss was not larger than 2.6 mm^2 in any experiment that we included in the data analysis (Fig. S1). We observed that both the temporal and the spatial distribution of VSD fluorescence response to limb stimulation changed within 1.5 h after stroke. After stroke responses spread relatively more to hindlimb territories as demonstrated in Fig. 2 and quantified below. In cases where we observed a partial loss of the forelimb map and an intact hindlimb area, we evaluated the spatial relationship between blood flow deficits and loss of function. The deficit in VSD map function extended 200–500 μm into regions of the prestroke forelimb map that contained some intact arteriole segments (Fig. 3*G* and Table S1), indicating a region that was perfused but nonfunctional, consistent with previous reports using less direct measures of activity such as Intrinsic Optical Signal (IOS) imaging (19).

After targeted stroke induction, we alternated monitoring VSD fluorescence and laser speckle maps to observe further changes in sensory-evoked depolarization and blood flow, usually for 4–6 h after induction of stroke. Recording of VSD responses was limited to this time range because the baseline fluorescence labeling decayed over time. Despite this confound, we did not observe significant changes in the temporal or spatial distribution of fluorescence signals as long as the laser speckle map did not change significantly either (i.e., no additional ischemia occurred). However, to ensure that the highest quality signals were studied we limited this study to data recorded 30–90 min after stroke induction. Data recorded before stroke within the same animal served as the control.

To quantitatively analyze changes in sensory-evoked VSD responses before and after stroke, we generated spatial profiles of the deficits observed by laser speckle microscopy and aligned them with the spatial profile of VSD responses (Fig. 3 *E* and *F*) as described in *SI Methods*. To distinguish between the immediate (peak) and delayed (off-peak) component of the VSD fluorescence response to limb stimulation, we divided the signal at (t = 100 ms), which provides a simple measure to quantify stroke-related changes in the response time course (Fig. S2). In the profiles of the immediate VSD responses (averaged 0–100 ms after limb stimulation), the hindlimb responses were centered on the negative wing and the forelimb responses on the positive wing of the profile under control conditions (Fig. 3*A*). After stroke, the immediate response to forelimb stimulation in the remaining forelimb area was reduced to <40% of before-stroke values, and its center was shifted into the hindlimb area (Fig. 3*B*).

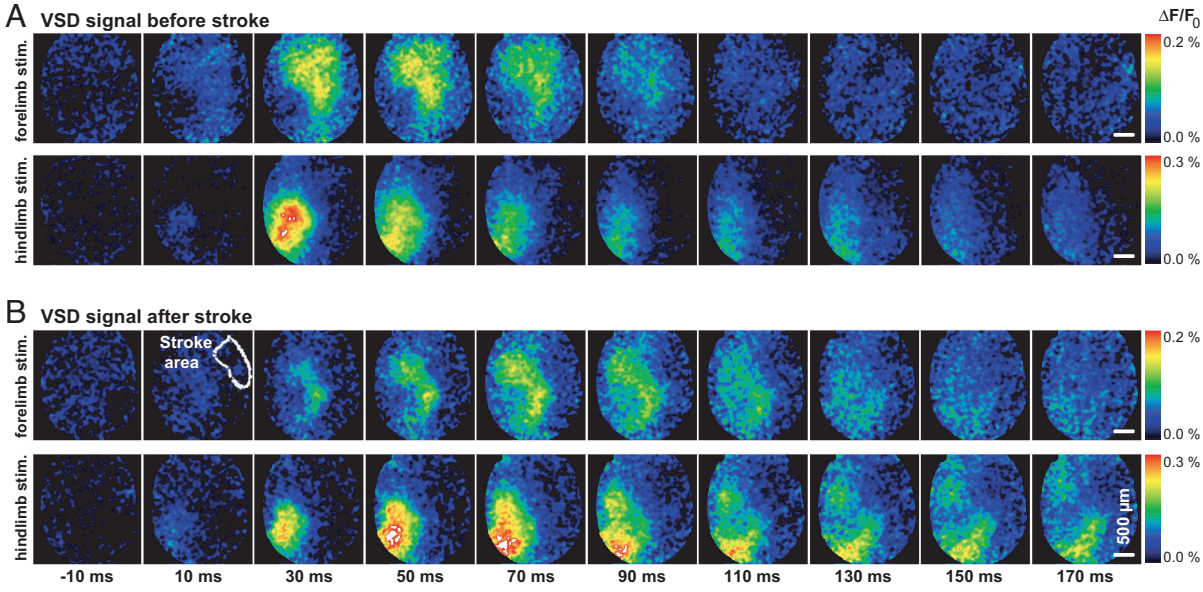

Fig. 2. The delayed component of the response to forelimb stimulation is centered in the hindlimb sensory map after forelimb area-targeted stroke. (*A*) VSD fluorescence signal response in the sensorimotor cortex to tactile stimulation of the forelimb (*Upper*) or hindlimb (*Lower*) 1 h before stroke induction. (*B*) VSD fluorescence signal responses as in *A*, 80 min after targeted photothrombotic focal stroke in the cortical area that represents the anterior forelimb map. (*Upper*, second from left) The stroke focus, determined by speckle imaging, is outlined. The delayed component of the response to forelimb stimulation (≥100 ms) is centered in areas that respond with short latency to hindlimb stimulation. Shown are averaged results of 20–40 trials.

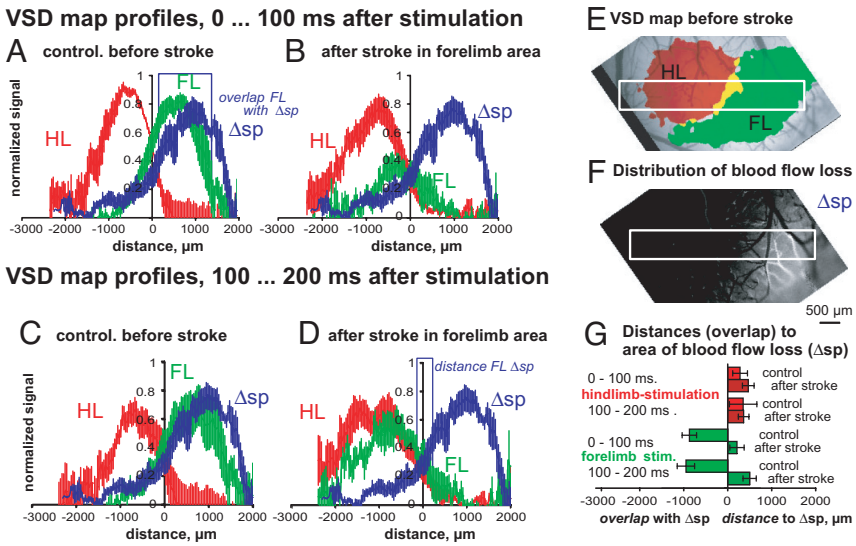

Fig. 3. Relationship between the loss of forelimb area blood flow and the redistribution of forelimb-stimulated activity within the sensorimotor cortex. (*A–D*) profiles of the VSD fluorescence responses to forelimb (FL, green) and hindlimb stimulation (HL, red) and the difference of speckle images of blood flow before and after stroke (ΔSp, blue). Profiles are aligned across animals to the right, lateral border, of the response to hindlimb stimulation. The profiles were then normalized separately for fore- and hindlimb stimulation to the peak response amplitudes before stroke. (*A*) Profile of the immediate response (0–100 ms after stimulation) before, and (*B*) 80 min after, focal stroke in the forelimb area. (*C*) Profile of the delayed response (100–200 ms after stimulation) before stroke and (*D*) 80 min after stroke. (*E*) Demonstration of the position used to obtain profiles of the VSD signal and (*F*) of the laser speckle difference images. To quantify the map shift, blue vertical lines (connected to each other at the top) indicate the lateral (*Right*) point of the half-maximum VSD response to forelimb stimulation and the medial (*Left*) point of the half-maximum of the speckle difference profile in *A* and *D*. We used these half-maximum points to define the border of the maps. (*G*) Quantitative comparison of overlap and distance between the borders of the limb-stimulated VSD signal and speckle maps. See Table S1 for further description and values plotted in *G*. Average data from 8 mice is shown.

The loss of signal in the forelimb area after stroke was expected given the observed change in speckle signal that we coplotted in with all profiles in Fig. 3 *A–D*. Looking at the delayed responses (which we averaged >100–200 ms after stimulation), responses to forelimb stimulation spread out into the hindlimb area (Fig. 3*C*). After stroke damage to much of the forelimb map, these delayed responses to forelimb stimulation were relatively preserved in the area that represents the hindlimb (Fig. 3*D*).

The centroids of these VSD fluorescence responses to forelimb simulation were shifted medially from the forelimb area into the hindlimb area within the sensorimotor cortex by ≈0.8–1.8 mm, depending on the time interval that was examined after stimulation (i.e., the shift was 805 μm for the interval 0–100 ms and 1,760 μm for 100–200 ms in average data from 8 mice; see Table S1).

To further examine the VSD fluorescence response to limb stimulation, we averaged data from 9 mice for 4 equivalent subregions of the somatosensory cortex limb areas: (*i*) the approximate center of the hindlimb (HL), (*ii*) the anterior part of the forelimb area affected by stroke (FL1), (*iii*) a region (usually the posterior-lateral part) of the forelimb area that was less affected by the targeted occlusion (FL2), and (*iv*) a region where responses to fore- and hindlimb stimulation overlapped (FL∩HL). Before stroke, responses measured after hindlimb or forelimb stimulation were greatest in the respective cortical areas with a response maximum within 100 ms after stimulation (Fig. 4 *A* and *C*). After stroke in the forelimb area, we recorded responses to limb stimulation (Fig. 4 *B* and *D*). In stroke cases after forelimb stimulation, the directly stroke-affected region of the forelimb area (FL1) did not show responses to limb stimulation. However, forelimb-stimulated responses were still present in nearby areas that were not ischemic (after stroke), including hindlimb regions, posterior forelimb areas (FL2), and regions of hind- and forelimb response overlap (FL∩HL). In these regions after stroke, the response kinetics were slowed in average data plots (Fig. 4*B*). Response amplitudes were blunted in FL2 and FL∩HL areas, although interestingly forelimb-stimulated responses that were present in the HL area were not reduced (Fig. 4*B*). These average data suggest that residual FL-stimulated activity present in HL regions is resistant to the effects of acute stroke, despite a large reduction in response at

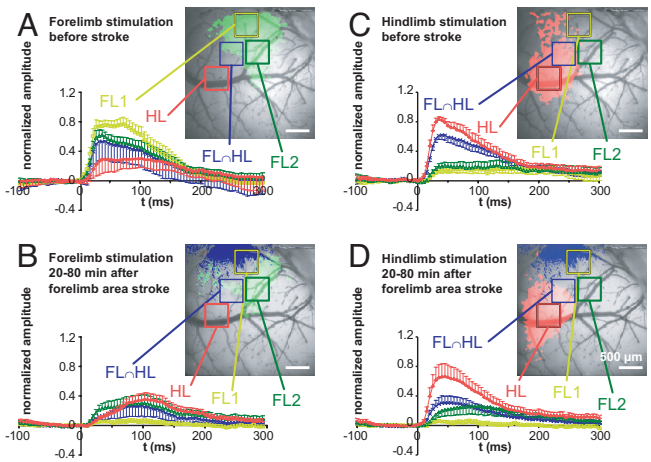

Fig. 4. Stroke targeted to the center of the forelimb area spares delayed forelimb responses that spread to the hindlimb area. (*A–D*) Temporal plots of the VSD response to fore or hindlimb stimulation, each with an image of 1 example showing the areas from which we determined the time courses. (*A* and *B*) Plot of VSD response to forelimb stimulation before (*A*) and after (*B*) stroke. (*C* and *D*) Plots of VSD response to hindlimb stimulation before (*C*) and after (*D*) stroke. In the image in *B* and *D*, loss of blood flow as determined by change of laser speckle signal is indicated in blue to display the ischemic area (blue shaded). VSD signals were averaged for 0.25-mm^2 regions of interest and normalized, separately for fore- and hindlimb stimulation, to the peak maximum of response amplitudes before stroke. Averaged data from 9 mice is shown.

NEUROSCIENCE

the FL map center (FL1). In addition, we observed that the posterior part of the forelimb representation (FL2) can maintain responsiveness even if the anterior part of the map is lost.

To further assess the effect of stroke on FL-stimulated activity in nearby regions we statistically compared parameters for response amplitude and kinetics between animals. As expected from the average intensity plots (Fig. 4) stroke directed at the FL area largely blocked the FL-stimulated response in FL1, but only partially affected nearby FL2 and the FL/HL overlap area when both the peak, immediate, and delayed responses were measured (Fig. S2 *A–D*). The time to peak VSD response was significantly slowed in the case of FL-stimulated VSD responses that were recorded in the HL area, and the rise time also tended to be longer (see Fig. S2 *E* and *F*). Consistent with a FL area-directed stroke, HL-stimulated VSD responses (measured in the HL map center) were not significantly affected.

Discussion

Remarkably, the mammalian brain can recover from unilateral cortical lesions through remapping of lost function (12, 28). We have examined changes to mouse somatosensory cortex maps in the first hours after photothrombotic stroke targeted to a subset of the forelimb area. We report that even within these short times after ischemia, the brain possesses 2 key features of remapping that facilitate the formation of new functional circuits during the following weeks to months. First, we show that partial sensory maps can exist if stroke is targeted to a subset of a cortical domain. Second, we show that intracortical connections exist that allow redistribution of sensory evoked depolarization into functionally related regions of cortex within minutes.

Blood Flow and Sensory Map Function. Previously, we (19) assessed relationships between local blood flow and sensory-evoked activity within the first few hours after stroke by using speckle and IOS imaging (29, 30). We reported a 300-μm wide area where blood flow is present, but not sensory-evoked responses (19). These studies of IOS hemodynamic responses, although informative, were potentially difficult to interpret because the response requires blood flow. In support of this work (19), we now show using VSD imaging that changes in local blood flow predict deficits in sensory-evoked depolarization, with the exception of a 200–500 μm wide area where blood flow was present, but little or no sensory-evoked activity occurred. Previous 2-photon imaging of GFP-labeled neurons indicated that these perfused, yet functionally silent, areas contain neurons with morphologically intact dendrites (19). Here, we did not combine VSD imaging with 2-photon imaging of dendritic structure since we cannot rule out phototoxic side effects caused by prolonged exposure to strong 2-photon excitation laser light in presence of VSD. Similarly, we avoided recording IOS maps after incubation of the cortex with VSD, because they would require long periods (>15 min) of bright red light exposure and potentially the formation of phototoxic products.

Partial Sensory Map Function After Targeted Ischemia. By targeting surface arteriole branches to block blood flow (19, 25, 27), we induced focal strokes that knocked out sensory-evoked depolarization within a subset of the forelimb area. This result suggests that one cortical subregion is not necessarily dependent on another for proper registration of sensory stimuli. It also suggests that somatosensory signals can be processed despite some degree of ischemic damage through the use of residual ascending or horizontal connections. Previously, we analyzed the structural integrity of layer V cortical neurons 2–10 h after photothrombotic stroke in the somatosensory limb area of the cortex and found that axonal and dendritic circuitry or somata, located 300 μm outside of an ischemic zone, can be relatively free of structural damage or commitment to cell death pathways (31). It is conceivable that in regions with partial map function, restoration of function through compensatory rewiring over days to weeks may be facilitated since some thalamic connections and intracortical connections are apparently still present hours after stroke. Our present work suggests that previous observations of partial IOS map function after stroke (19) were not attributable to limitations of imaging hemodynamic signals, but reflect retention of partial function despite stroke (32, 33). Other previous work supports the observation that after an incomplete lesion, partial cortical function can be maintained (34, 35), depending on the extent of the loss.

Relationship Between Rapid and Delayed Changes to Sensory Maps After Stroke. Although we focus here on changes to sensory maps in the first hours after targeted occlusion, we have previously studied structural plasticity and endpoint changes to sensory maps 1–8 weeks after stroke (2–4). Our results are consistent with a model where the spatial extent of initial stroke damage, and the distribution of synaptic connections that survive the insult, determine, which tissues are available to form new cortical representations in the recovering brain. VSD imaging reveals a surprising degree of intracortical connectivity between related regions of cortex such as sensory and motor areas within tens of milliseconds (18). At longer time points after sensory stimulation (100–300 ms), voltage-sensitive dye imaging reveals propagation of depolarization throughout much of the hemisphere. Conceivably, relatively diffuse sensory signaling could be strengthened over the days, weeks, and months over which recovery from stroke damage occurs (7, 36–38). We suggest that the mammalian brain initially relies on some preserved connections from afferent sensory pathways to route signals around injured components of sensory maps. Although this redistribution of cortical activity apparently takes place within the first hours after stroke in the forelimb area, in this model 1 week later, the somatosensory cortex has little detectable response to forelimb stimulation (21). It is conceivable that over a week's time factors such as inflammation (39–41) and byproducts of ongoing cell death (within the core) limit sensory-evoked activation. Alternatively, these conditions may interfere with the detection of VSD responses at 1 week after stroke. Two weeks after stroke, individual layer II neurons in affected forelimb territories and peri-infarct areas do respond, but with reduced limb specificity (4). Eight weeks after focal stroke, forelimb cortex responses have remapped to neighboring motor and sensory hindlimb areas with prolonged kinetics (21), and the limb specificity of individual neurons (4) is substantially recovered.

Possible Mechanisms of Rapid Redistribution of Map Function. Previous studies suggest that neurons become hyperexcitable after stroke through changes in excitation and inhibition balance. Electrophysiological studies for acute slices showed that oxygen deprivation causes an immediate reduction of GABAergic synaptic transmission (42, 43). At the same time, the expression of functional $GABA_A$ receptors is reduced (44, 45), synaptic glutamate release becomes elevated (46, 47), and NMDA receptor activity is enhanced (45, 48). Taken together, these effects lead to hyperexcitability and may facilitate propagation of residual sensory responses to sites away from damaged maps (36). Excitation-inhibition balance could also change as a result of a loss of surround inhibition (1, 47, 49, 50), which leads to enhanced out-of-territory responses. These altered electrophysiological properties could induce potentiation of excitatory inputs in the peri-infarct cortex within the first hour after stroke (16) and form an environment suitable for later rewiring (3, 4, 36, 37, 51) that correlates with functional reorganization (1, 49, 50, 52). Consistent with a hyperexcitable cortex, within the first week after ischemic stroke in rats, the size of perilesional receptive fields increases (33). Regarding structural mechanisms

of early changes to circuits hours after stroke, synaptogenesis is unlikely since the formation of new synaptic connections in the adult cortex would likely take longer (53). Therefore, existing but less active connections (36) could mediate short-term reorganization of the somatosensory cortex after focal ischemia. These events could underlie some forms of rapid behavioral compensation and direct future synaptically mediated stroke recovery at later time points.

How Are Sensory Signals Preserved Despite Stroke Damage? We find that the initial short latency depolarizing responses that occur within the center of cortical maps are the most sensitive to ischemic damage. It is likely that these sharply tuned short latency responses have little redundancy. In contrast, longer latency responses, which spread throughout the hemisphere, are relatively less sensitive to ischemic damage. One question is how these slower signals are relayed if the sites of their initial thalamic inputs to the cortex are lost. The first explanation would be partial preservation of limb-specific sensory maps. The second would be latent subthreshold (17, 54), ascending or horizontal cortical connections that eventually more circuitously route sensory signals to related brain regions. We propose that these circuits are not directly affected by stroke and relay information to regions close to the infarct (Fig. 5). The potentially indirect nature of these circuits would explain the observation that the delayed responses are more effectively rerouted after stroke (Fig. 4).

In summary, we reveal a remarkable capacity of the brain to deal with focal damage over short time scales. We hope these findings may help to suggest strategies by which rehabilitation and therapy after stroke can be geared to make the best use of residual circuits leading to remapping of sensory responses.

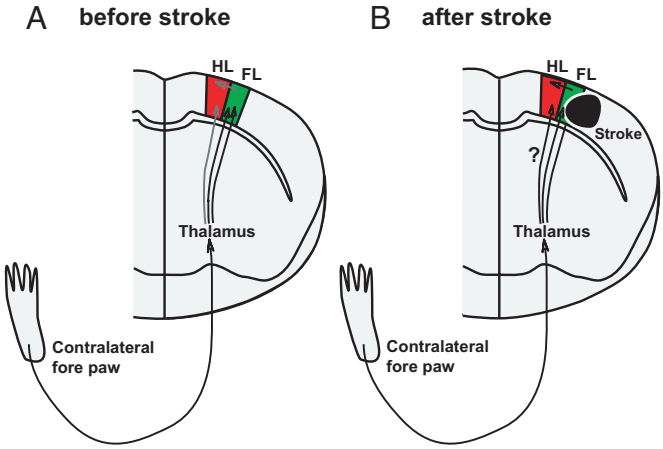

Fig. 5. Schematic illustration of rapid sensory response redistribution mechanisms for somatosensory cortex function. (*A*) Control (before stroke). Sensory signals coming from the contralateral (left) front paw are first processed within the contralateral thalamus, routed to the primary somatosensory cortex (FL, green), and then to nearby cortical regions such as the sensory HL area. (*B*) After stroke in the FL area, thalamocortical connections carrying FL-derived signals are lost, which could enhance the importance of intracortical and thalamocortical connections that bring FL signals to areas that represent the HL in the sensorimotor cortex. This scheme may explain the stroke-related spatial redistribution of cortical activity that we observed (Fig. 3). The smaller number of intact thalamocortical connections, or the circuitous route the signals take, may explain why the responses to forelimb stimulation observed in off-target areas such as hindlimb cortex are slower after stroke (Fig. 4).

Materials and Methods

For methodological details see *SI Methods*. Urethane-anesthetized mice aged 2–5 months and weighing 24–32 g were used for all experiments. Animal protocols were approved by the University of British Columbia Animal Care Committee and were consistent with Canadian Council for Animal Care guidelines. For in vivo imaging, a 3 × 3 mm craniotomy was performed over the right somatosensory cortex as described briefly in *SI Methods* and in more detail in (19, 55). The dura was carefully removed in the craniotomy window, allowing topically applied voltage-sensitive dye (RH1692; Optical Imaging) to better access the somatosensory cortex (20, 22) for 90 min. VSD signal responses to stimulation were calculated as the normalized difference to the average baseline recorded before stimulation ($\Delta F/F_0$). To periodically assess blood flow, we imaged laser speckle contrast (24) as described in *SI Methods*. Focal stroke was induced in surface vessels as we described (19, 25) by the photothrombosis with Rose Bengal (26). We injected the photosensitizing dye (Na^+ salt, Sigma R3877; diluted to 10 mg/mL in Hepes-buffered saline) into the tail vein to a final dosage of 30 μg/g mouse body weight. Within 10 min after injection, we targeted individual surface arterioles to induce photothrombotic blockage of blood flow using a 0.7–1.4 mW (measured at the objective back aperture) 532-nm beam from a diode pumped laser (Beta Electronics MGM-20) as described in detail (25).

ACKNOWLEDGMENTS. We thank Pumin Wang for his excellent mouse surgeries, Heidi Erb and Alexander Goroshkov for technical support, Khashayar Golbaz for help with data analysis, and Craig Brown for critical reading of the manuscript. This work was supported by operating grants to T.H.M. from Canadian Institutes of Health Research (MOP49586) and the Canadian Stroke Network, and by a postdoctoral fellowship to M.H.M. from Michael Smith Foundation for Health Research.

1. Carmichael ST (2006) Cellular and molecular mechanisms of neural repair after stroke: Making waves. *Ann Neurol* 59:735–742.
2. Brown CE, et al. (2007) Extensive turnover of dendritic spines and vascular remodeling in cortical tissues recovering from stroke. *J Neurosci* 27:4101–4109.
3. Brown CE, Murphy TH (2007) Livin' on the edge: Imaging dendritic spine turnover in the peri-infarct yone during ischemic stroke and recovery. *Neuroscientist* 14:139–146.
4. Winship IR, Murphy TH (2008) In vivo calcium imaging reveals functional rewiring of single somatosensory neurons after stroke. *J Neurosci* 28:6592–6606.
5. Dijkhuizen RM, et al. (2001) Functional magnetic resonance imaging of reorganization in rat brain after stroke. *Proc Natl Acad Sci USA* 98:12766–12771.
6. Ramanathan D, Conner JM, Tuszynski MH (2006) A form of motor cortical plasticity that correlates with recovery of function after brain injury. *Proc Natl Acad Sci USA* 103:11370–11375.
7. Bütefisch CM (2004) Plasticity in the human cerebral cortex: Lessons from the normal brain and from stroke. *Neuroscientist* 10:163–173.
8. Sanes JN, Donoghue JP (2000) Plasticity and primary motor cortex. *Annu Rev Neurosci* 23:393–415.
9. Garraghty PE, Pons TP, Kaas JH (1990) Ablations of areas 3b (SI proper) and 3a of somatosensory cortex in marmosets deactivate the second and parietal ventral somatosensory areas. *Somatosens Mot Res* 7:125–135.
10. Maggiolini E, Viaro R, Franchi G (2008) Suppression of activity in the forelimb motor cortex temporarily enlarges forelimb representation in the homotopic cortex in adult rats. *Eur J Neurosci* 27:2733–2746.
11. Nudo RJ, Wise BM, SiFuentes F, Milliken GW (1996) Neural substrates for the effects of rehabilitative training on motor recovery after ischemic infarct. *Science* 272:1791–1794.
12. Xerri C, Merzenich MM, Peterson BE, Jenkins W (1998) Plasticity of primary somatosensory cortex paralleling sensorimotor skill recovery from stroke in adult monkeys. *J Neurophysiol* 79:2119–2148.
13. Jones TA, Kleim JA, Greenough WT (1996) Synaptogenesis and dendritic growth in the cortex opposite unilateral sensorimotor cortex damage in adult rats: A quantitative electron microscopic examination. *Brain Res* 733:142–148.
14. Carmichael ST, Chesselet MF (2002) Synchronous neuronal activity is a signal for axonal sprouting after cortical lesions in the adult. *J Neurosci* 22:6062–6070.
15. Risedal A, Zeng J, Johansson BB (1999) Early training may exacerbate brain damage after focal brain ischemia in the rat. *J Cereb Blood Flow Metab* 19:997–1003.
16. Fujioka H, Kaneko H, Suzuki SS, Mabuchi K (2004) Hyperexcitability-associated rapid plasticity after a focal cerebral ischemia. *Stroke* 35:e346–e348.
17. Berger T, et al. (2007) Combined voltage and calcium epifluorescence imaging *in vitro* and *in vivo* reveals subthreshold and suprathreshold dynamics of mouse barrel cortex. *J Neurophysiol* 97:3751–3762.
18. Ferezou I, et al. (2007) Spatiotemporal dynamics of cortical sensorimotor integration in behaving mice. *Neuron* 56:907–923.
19. Zhang S, Murphy TH (2007) Imaging the impact of cortical microcirculation on synaptic structure and sensory-evoked hemodynamic responses *in vivo*. *PLoS Biol* 5:e119.
20. Shoham D, et al. (1999) Imaging cortical dynamics at high spatial and temporal resolution with novel blue voltage-sensitive dyes. *Neuron* 24:791–802.
21. Brown CE, et al. (2009) In vivo voltage-sensitive dye imaging in adult mice reveals that somatosensory maps lost to stroke are replaced over weeks by new structural and functional circuits with prolonged modes of activation within both the peri-infarct zone and distant sites. *J Neurosci* 29:1719–1734.

22. Petersen CC, Grinvald A, Sakmann B (2003) Spatiotemporal dynamics of sensory responses in layer 2/3 of rat barrel cortex measured *in vivo* by voltage-sensitive dye imaging combined with whole-cell voltage recordings and neuron reconstructions. *J Neurosci* 23:1298–1309.
23. Grinvald A, Hildesheim R (2004) VSDI: A new era in functional imaging of cortical dynamics. *Nat Rev Neurosci* 5:874–885.
24. Briers JD, Richards G, He XW (1999) Capillary blood flow monitoring using laser speckle contrast analysis (LASCA). *J Biomed Opt* 4:164–175.
25. Sigler A, Goroshkov A, Murphy TH (2007) Hardware and methodology for targeting single brain arterioles for photothrombotic stroke on an upright microscope. *J Neurosci Methods* 170:35–44.
26. Watson BD, et al. (1985) Induction of reproducible brain infarction by photochemically initiated thrombosis. *Ann Neurol* 17:497–504.
27. Schaffer CB, et al. (2006) Two-photon imaging of cortical surface microvessels reveals a robust redistribution in blood flow after vascular occlusion. *PLoS Biol* 4:e22.
28. Weiller C (1998) Imaging recovery from stroke. *Exp Brain Res* 123:13–17.
29. Frostig RD, Lieke EE, Ts'o DY, Grinvald A (1990) Cortical functional architecture and local coupling between neuronal activity and the microcirculation revealed by *in vivo* high-resolution optical imaging of intrinsic signals. *Proc Natl Acad Sci USA* 87:6082–6086.
30. Grinvald A, et al. (1986) Functional architecture of cortex revealed by optical imaging of intrinsic signals. *Nature* 324:361–364.
31. Enright LE, Zhang S, Murphy TH (2007) Fine mapping of the spatial relationship between acute ischemia and dendritic structure indicates selective vulnerability of layer V neuron dendritic tufts within single neurons *in vivo*. *J Cereb Blood Flow Metab* 27:1185–1200.
32. Dancause N, et al. (2006) Effects of small ischemic lesions in the primary motor cortex on neurophysiological organization in ventral premotor cortex. *J Neurophysiol* 96:3506–3511.
33. Reinecke S, Dinse HR, Reinke H, Witte OW (2003) Induction of bilateral plasticity in sensory cortical maps by small unilateral cortical infarcts in rats. *Eur J Neurosci* 17:623–627.
34. Jain N, Qi HX, Collins CE, Kaas JH (2008) Large-scale reorganization in the somatosensory cortex and thalamus after sensory loss in macaque monkeys. *J Neurosci* 28:11042–11060.
35. Garraghty PE, Hanes DP, Florence SL, Kaas JH (1994) Pattern of peripheral deafferentation predicts reorganizational limits in adult primate somatosensory cortex. *Somatosens Mot Res* 11:109–117.
36. Di Filippo M, et al. (2008) Plasticity and repair in the post-ischemic brain. *Neuropharmacology* 55:353–362.
37. Carmichael ST (2003) Plasticity of cortical projections after stroke. *Neuroscientist* 9:64–75.
38. Nudo RJ (1999) Recovery after damage to motor cortical areas. *Curr Opin Neurobiol* 9:740–747.
39. Hossmann KA (1994) Viability thresholds and the penumbra of focal ischemia. *Ann Neurol* 36:557–565.
40. Jones TH, et al. (1981) Thresholds of focal cerebral ischemia in awake monkeys. *J Neurosurg* 54:773–782.
41. Block F, Dihné M, Loos M (2005) Inflammation in areas of remote changes following focal brain lesion. *Prog Neurobiol* 75:342–365.
42. Centonze D, et al. (2001) Adenosine-mediated inhibition of striatal GABAergic synaptic transmission during *in vitro* ischaemia. *Brain* 124:1855–1865.
43. Luhmann HJ, Mudrick-Donnon LA, Mittmann T, Heinemann U (1995) Ischaemia-induced long-term hyperexcitability in rat neocortex. *Eur J Neurosci* 7:180–191.
44. Qü M, et al. (1998) Bihemispheric reduction of $GABA_A$ receptor binding following focal cortical photothrombotic lesions in the rat brain. *Brain Res* 813:374–380.
45. Hagemann G, et al. (1998) Increased long-term potentiation in the surround of experimentally induced focal cortical infarction. *Ann Neurol* 44:255–258.
46. Benveniste H, Drejer J, Schousboe A, Diemer NH (1984) Elevation of the extracellular concentrations of glutamate and aspartate in rat hippocampus during transient cerebral ischemia monitored by intracerebral microdialysis. *J Neurochem* 43:1369–1374.
47. Wang JH (2003) Short-term cerebral ischemia causes the dysfunction of interneurons and more excitation of pyramidal neurons in rats. *Brain Res Bull* 60:53–58.
48. Kozlowski DA, Schallert T (1998) Relationship between dendritic pruning and behavioral recovery following sensorimotor cortex lesions. *Behav Brain Res* 97:89–98.
49. Kolb B, et al. (2007) Growth factor-stimulated generation of new cortical tissue and functional recovery after stroke damage to the motor cortex of rats. *J Cereb Blood Flow Metab* 27:983–997.
50. Nudo RJ (2006) Mechanisms for recovery of motor function following cortical damage. *Curr Opin Neurobiol* 16:638–644.
51. Wiessner C, et al. (2003) Anti-Nogo-A antibody infusion 24 hours after experimental stroke improved behavioral outcome and corticospinal plasticity in normotensive and spontaneously hypertensive rats. *J Cereb Blood Flow Metab* 23:154–165.
52. Zepeda A, et al. (2004) Functional reorganization of visual cortex maps after ischemic lesions is accompanied by changes in expression of cytoskeletal proteins and NMDA and GABA(A) receptor subunits. *J Neurosci* 24:1812–1821.
53. Zito K, Svoboda K (2002) Activity-dependent synaptogenesis in the adult Mammalian cortex. *Neuron* 35:1015–1017.
54 Smits E, Gordon DC, Witte S, Rasmusson DD, Zarzecki P (1991) Synaptic potentials evoked by convergent somatosensory and corticocortical inputs in raccoon somatosensory cortex: Substrates for plasticity. *J Neurophysiol* 66:688–695.
55. Kleinfeld D, Denk W (2000) in *Imaging Neurons: A Laboratory Manual*, eds Yuste R, Lanni F, Konnerth A (Cold Spring Harbor Lab Press, Cold Spring Harbor, NY), pp 23.15–23.21.

Supporting Information

Sigler et al. 10.1073/pnas.0812695106

SI Methods

Animal Model. Adult, urethane-anesthetized mice aged 2–5 months and weighing 24–32 g were used for all experiments. Animal protocols were approved by the University of British Columbia Animal Care Committee and were consistent with Canadian Council for Animal Care guidelines. Briefly, anesthesia was induced with urethane (0.12% wt/wt) and body temperature was maintained at 37 ± 0.5 °C by using a heating pad and feedback regulation from a rectal temperature probe. A 3 × 3 mm craniotomy was performed over the right somatosensory cortex. The skull was fastened to a stainless steel plate (1) with cyanoacrylate glue and dental cement as in ref. 2. Assessment of blood oxygen saturation (on average >90%), heart rate (400–600 beats/min), and breathing rate (≈200 breaths/min) in a subset of animals indicated that under the conditions we used for imaging, physiological parameters were relatively constant over the course of our experiments. All animals were under urethane anesthesia and breathing air as described previously (2). Hydration was maintained by i.p. injection of saline (100–200 μL) with 20 mM glucose at 1–2-h intervals.

VSD Imaging. For in vivo voltage-sensitive dye (VSD) experiments, the dura was carefully removed in the craniotomy window, allowing the dye to better access the somatosensory cortex (3, 4). The dye, RH1692 (Optical Imaging), was dissolved in the Hepes-buffered saline to an optical density of 4.0–7.0 (measured at 550 nm) and topically applied to the exposed cortex, allowing it to diffuse into the tissue for 90 min. To minimize movement artifacts, the brain was covered with 1–1.5% agarose made in physiological saline (Type 3-A Sigma; A9793) and sealed with a glass coverslip.

For VSD data collection, 12-bit image frames were captured every 5.0 or 6.6 ms with a digital camera (1M60 Dalsa) mounted on an upright Olympus BX51 microscope and an EPIX E1DB frame grabber with XCAP 2.2 imaging software (EPIX, Inc.). VSD fluorescence was excited at 627 nm with LED light (Luxeon K2, Philips Lumileds), filtered with a fluorescence filter set as outlined previously (4, 5), and focused 300 μm below the surface with an Olympus XL Fluor 4×/340 NA 0.28 long distance lens. Images were collected for 200 ms before and 500 ms after tactile stimulation of the contralateral fore- or hindlimb as single pulses with 5-ms length through a custom-made moving device consisting of a piezoelectric bending actuator (Q220-AY-203YB, Piezo Systems) driven by an isolated pulse stimulator (Model 2100, AM Systems). We processed the recorded data by using the image analysis program ImageJ (National Institute of Mental Health, Bethesda, MD) with a custom-written plug-in. VSD signal responses to stimulation were calculated as the normalized difference to the average baseline recorded before stimulation ($\Delta F/F_0$). This method allowed us to remove offsets, which may be caused by bleaching and diffusion of VSD fluorophores and by potential changes in background fluorescence due to other sources such as spontaneous activity as long as the signal-to-noise ratio is large enough to allow accurate determination. To minimize the contribution of these and other artifacts to the result, data for at least 10, typically 30, sets of stimulation trials were averaged and normalized to the data for trials that were recorded without stimulation.

Multigroup comparisons were made by using an ANOVA with post-hoc tests. A P value ≤0.05 was considered statistically significant, except for multiple post-hoc comparisons; in that case the Bonferroni correction was used to set the α-level. All data are expressed as the mean ± SE.

Profile Plots. To quantitatively analyze changes in sensory-evoked VSD responses before and after stroke, we generated spatial profiles of the deficits observed by laser speckle microscopy and aligned them with the spatial profile of VSD responses (Fig. 3 *E* and *F*). VSD signal profiles were normalized, separately for fore- and hindlimb stimulation, to the peak maximum of response amplitudes before stroke. The right, lateral edge of the response to hindlimb stimulation (defined as the point of half-maximal signal at the side that is bordering the forelimb response within the profile) before stroke served as the zero point of alignment for data from each mouse. Using this functional landmark, we were able to align data from different animals significantly better than with an absolute anatomical landmark based on bregma position.

Stroke Model. Focal stroke was induced as we described (2, 6) by using the Rose Bengal photothrombosis model (7). We injected the photosensitizing dye (Na^+ salt, Sigma R3877; diluted to 10 mg/mL in Hepes-buffered saline) into the tail vein to a final dosage of 30 μg/g mouse body weight. Within 10 min after injection, we targeted individual surface arterioles to induce photothrombotic blockage of blood flow using a 0.7–1.4 mW (measured at the objective back aperture) 532-nm beam from a diode-pumped laser (Beta Electronics MGM-20) that was coupled to the microscope's epifluorescence light path and focused into a spot through a 40×, 0.8 NA water immersion lens as described in detail (6). Individual arterioles supplying the forelimb or hindlimb areas were identified from their appearance and position within the map of somatosensory forelimb representation in VSD imaging. To reduce the ability of the brain to support the targeted area based on redundant paths of blood flow, vessels were targeted at multiple points for repeated periods of ≈1–2 min (2, 6).

Laser Speckle Imaging. To periodically assess blood flow, we imaged laser speckle contrast as similarly described (2, 6). Laser-speckle imaging of blood flow is based on blurring of interference patterns of scattered laser light, whereas the blurring is caused by the flowing of blood cells (8–10). For illumination, a 784-nm 32-mW StockerYale SNF-XXX-785S-35 laser (Stocker & Yale) with an Edmund anamorphic beam expander T47274 (Edmund Optics) was held directly on a micromanipulator at an angle of 30° and directed at the brain surface that was enclosed by a coverslip and agarose and viewed with a 4 × 0.075 NA objective. We recorded images with a Dalsa M60 Pantera camera (Dalsa) mounted on the upright microscope used for photoactivation. Typically, we collected 30–100 images at 10 Hz by using a 10-ms exposure. Individual images of variance were created in ImageJ (National Institute of Mental Health, Bethesda, MD) using its 2-dimensional variance filter (3 × 3 or 5 × 5 pixel kernel size, 3.47 μm/pixel). Following variance filtering, all images were averaged, and a single 32-bit image of the standard deviation was produced by taking the square root of the averaged variance image. The standard deviation image was then divided by the mean of all of the raw images to help correct for uneven illumination and to create an image of speckle contrast (standard deviation/mean).

1. Kleinfeld D, Denk W (2000) in *Imaging Neurons*: *A Laboratory Manual*, eds Yuste R, Lanni F, Konnerth A. (Cold Spring Harbor Lab Press, Cold Spring Harbor, NY), pp 23.15–23.21.
2. Zhang S, Murphy TH (2007) Imaging the impact of cortical microcirculation on synaptic structure and sensory-evoked hemodynamic responses *in vivo*. *PLoS Biol* 5:e119.
3. Shoham D, et al. (1999) Imaging cortical dynamics at high spatial and temporal resolution with novel blue voltage-sensitive dyes. *Neuron* 24:791–802.
4. Petersen CC, Grinvald A, Sakmann B (2003) Spatiotemporal dynamics of sensory responses in layer 2/3 of rat barrel cortex measured *in vivo* by voltage-sensitive dye imaging combined with whole-cell voltage recordings and neuron reconstructions. *J Neurosci* 23:1298–1309.
5. Ferezou I, Bolea S, Petersen CC (2006) Visualizing the cortical representation of whisker touch: Voltage-sensitive dye imaging in freely moving mice. *Neuron* 50:617–629.
6. Sigler A, Goroshkov A, Murphy TH (2007) Hardware and methodology for targeting single brain arterioles for photothrombotic stroke on an upright microscope. *J Neurosci Methods* 170:35–44.
7. Watson BD, et al. (1985) Induction of reproducible brain infarction by photochemically initiated thrombosis. *Ann Neurol* 17:497–504.
8. Briers JD, Webster S (1996) Laser Speckle contrast analysis (LASCA): A nonscanning, full-field technique for monitoring capillary blood flow. *J Biomed Opt* 1: 174–179.
9. Briers JD, Richards G, He XW (1999) Capillary blood flow monitoring using laser speckle contrast analysis (LASCA). *J Biomed Opt* 4:164–175.
10. Dunn AK, Bolay H, Moskowitz MA, Boas DA (2001) Dynamic imaging of cerebral blood flow using laser speckle. *J Cereb Blood Flow Metab* 21:195–201.

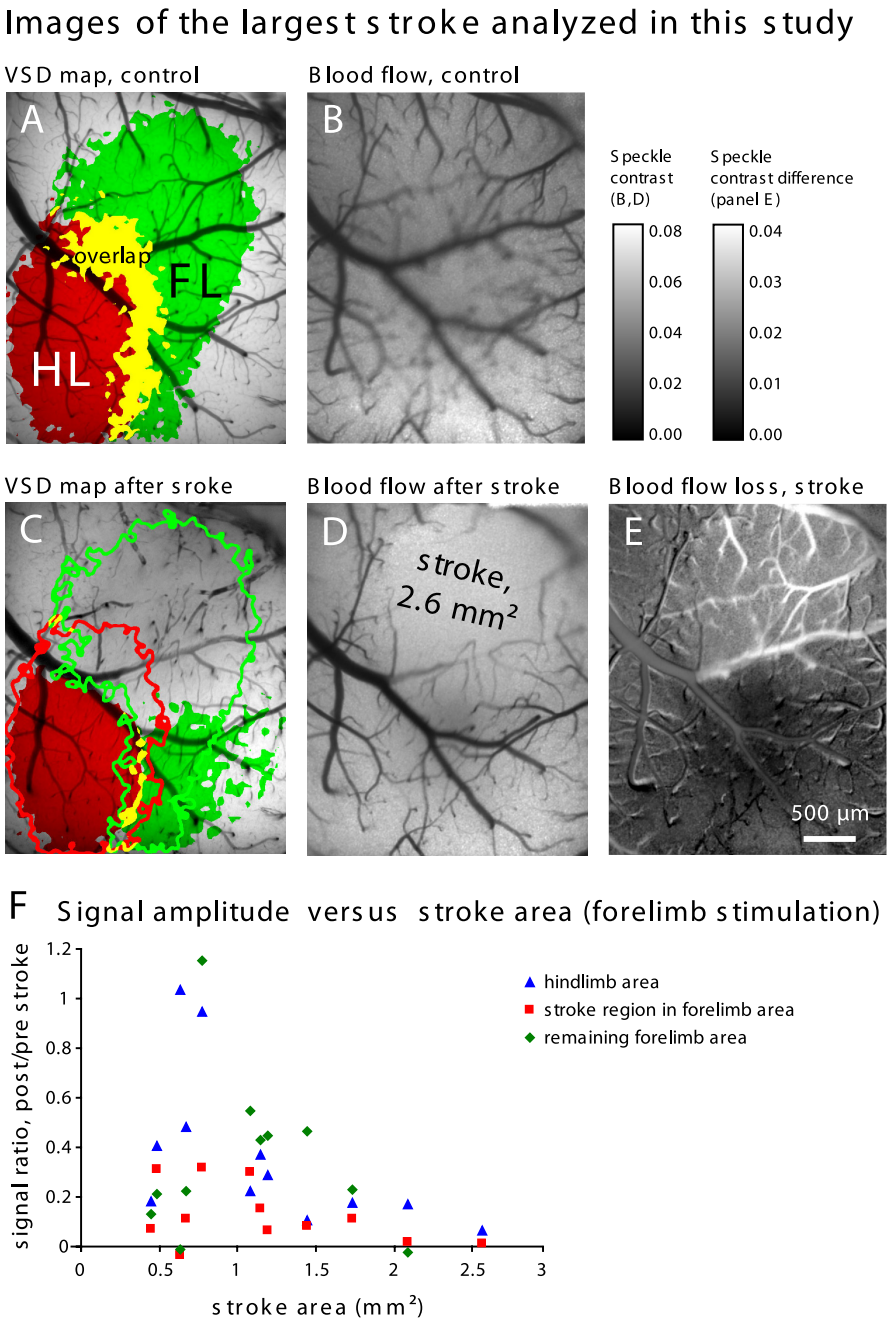

Fig. S1. Criteria for standardization of stroke area between animals. Focal ischemic stroke are induced by photothrombotic blockage of blood vessels in the forelimb area of the mouse somatosensory cortex. For this study, we induced focal photothrombotic stroke in the somatosensory cortex of mice by targeting blood vessels in the area that represents the forelimb. (*A–E*) Images of somatosensory cortex after craniotomy before (*A* and *B*) and after (*C* and *D*) induction of a relatively large stroke. (*A*) Maps of voltage sensitive dye (VSD) fluorescence changes indicating depolarization in the sensorimotor cortex in response to stimulation of forelimb (FL, green), hindlimb (HL, red), and the overlap of forelimb and hindlimb map (yellow). (*B*) Laser speckle image to determine blood flow of the same region of the somatosensory cortex; dark stain indicates blood flow (reduced speckle contrast). Speckle contrast was determined as ratio of standard deviation/mean as described in *SI Methods*. (*C*) Maps of VSD fluorescence as in *A* after photothrombotic stroke. The red and green outlines indicate areas of response to hindlimb and forelimb stimulation. (*D*) Laser speckle image after stroke indicates an area of blood flow loss (less darker stain, higher speckle variance) due to stroke in forelimb area. (*E*) Difference of image in *D* and *B*. Bright stain indicates blood flow loss. The area covered by this stroke is approximately 2.6 mm^2, which is the largest size of a stroke that we used for this study. (*F*) Relationship of VSD fluorescence signal amplitude to the size of stroke area. Plotted is the ratio of peak amplitudes of responses to forelimb stimulation, before and after stroke, in relation to the size of the stroke area.

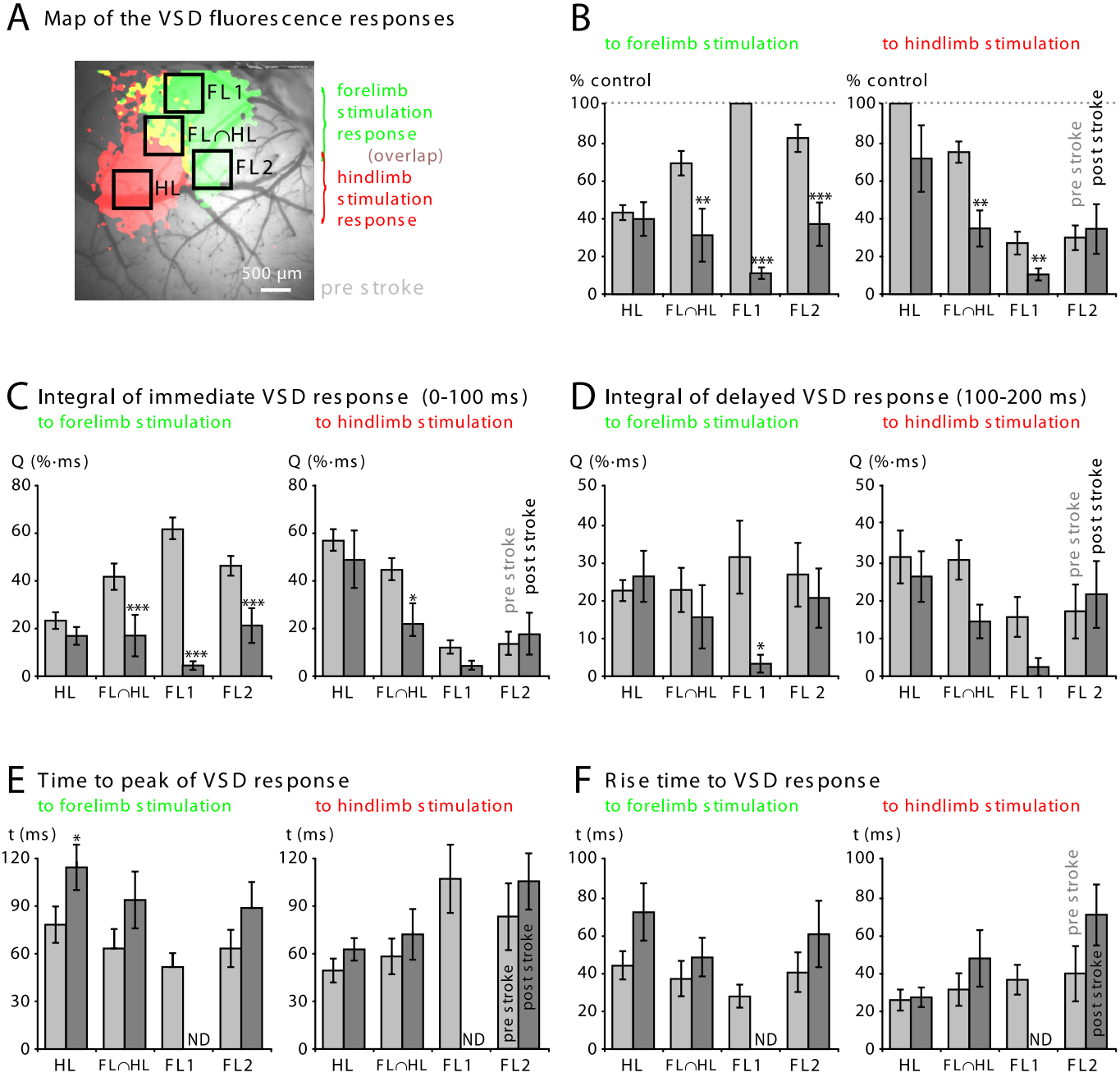

Fig. S2. Quantification of kinetics and amplitude of VSD response to stimulation of forelimb or hindlimb before and after stroke. Based on data also shown in Fig. 4, we determined amplitude, amplitude integral, and rise time of VSD fluorescence responses in the sensorimotor cortex to tactile limb stimulation. (*A*) Map of VSD fluorescence signal responses to tactile stimulation, indicating hindlimb (HL; red), forelimb (FL1, FL2; green) and overlap of forelimb and hindlimb areas (FL∩HL, yellow) within the sensorimotor cortex. (*B*) Peak amplitudes, normalized to control. For hindlimb stimulation, responses in hindlimb area (HL, before stroke) served as control. For forelimb stimulation, responses in the anterior forelimb area (FL1) were used for normalization instead. (*C* and *D*) Integral of the VSD response signal amplitude (area under the curve) for the immediate (t = 0–100 ms) and delayed component (t = 100–200 ms) of VSD responses. (*E*) Time to peak and (*F*) rise time of VSD responses. VSD signal intensities were averaged for regions of interest with an area of 0.25 mm^2 (n = 9 animals, $P < 0.05$).

Table S1. Spatial parameters of map changes after stroke targeted to the forelimb area

	Forelimb		Hindlimb	
Observation time	0–100 ms	100–200 ms	0–100 ms	100–200 ms
Shift of cortical limb representation after stroke, μm*	805 ± 186	1760 ± 213	114 ± 25.2	208 ± 122
Distance (negative/overlap) of limb representation to post-stroke areas of blood flow loss, μm†				
Before stroke	−955 ± 181	−1040 ± 218	305 ± 181	383 ± 340
After stroke	230 ± 177	545 ± 164	509 ± 145	513 ± 132

To quantify the localization changes in the cortical limb representation after stroke, we calculated profiles through the area of VSD fluorescence signal response as shown in Fig. 3. Profiles are aligned with the right, lateral border of the response to hindlimb stimulation (defined as the point of half maximal signal) prior to stroke serving as the zero point of alignment for data from each mouse. After focal stroke targeted to the forelimb, responses to forelimb stimulation center in the hindlimb area. Average of data taken from 8 mice.

*We measured the distance of the signal centroids in the plotted profile to determine the apparent shift of cortical limb representation for both the immediate (within the first 100 ms) and the delayed component (100–200 ms) of the VSD signals.

†Distance between the border of limb representation and the border of blood flow loss after stroke. Negative values indicate overlap (see graphics in Fig. 3). This was determined both for the immediate and the delayed components of response.